Inorg. Chem. **2006**, *45*, 10077–10087

Silver(I) Complexes of Fixed, Polytopic Bis(pyrazolyl)methane Ligands: Influence of Ligand Geometry on the Formation of Discrete Metallacycles and Coordination Polymers

Daniel L. Reger,* Russell P. Watson, and Mark D. Smith

Department of Chemistry and Biochemistry, University of South Carolina, Columbia, South Carolina 29208

Received July 14, 2006

Reactions of the arene-linked bis(pyrazolyl)methane ligands *m*-bis[bis(1-pyrazolyl)methyl]benzene, (*m*-$[CH(pz)_2]_2C_6H_4$, $\mathbf{L}_m$), *p*-bis[bis(1-pyrazolyl)methyl]benzene, (*p*-$[CH(pz)_2]_2C_6H_4$, $\mathbf{L}_p$), and 1,3,5-tris[bis(1-pyrazolyl)methyl]benzene (1,3,5-$[CH(pz)_2]_3C_6H_3$, $\mathbf{L}^3$) with AgX salts (pz = 1-pyrazolyl; X = BF_4^- or PF_6^-) yield two types of molecular motifs depending on the arrangement of the ligating sites about the central arene ring. Reactions of the *m*-phenylene-linked $\mathbf{L}_m$ with $AgBF_4$ and $AgPF_6$ afford complexes consisting of discrete, metallacyclic dications: $[Ag_2(\mu\text{-}\mathbf{L}_m)_2](BF_4)_2$ (**1**) and $[Ag_2(\mu\text{-}\mathbf{L}_m)_2](PF_6)_2$ (**2**). When the *p*-phenylene-linked $\mathbf{L}_p$ is treated with $AgBF_4$ and $AgPF_6$, acyclic, cationic coordination polymers are obtained: $\{[Ag(\mu\text{-}\mathbf{L}_p)]BF_4\}_\infty$ (**3**) and $\{[Ag(\mu\text{-}\mathbf{L}_p)]PF_6\}_\infty$ (**4**). Reaction of the ligand $\mathbf{L}^3$, containing three bis(pyrazolyl)methane units in a meta arrangement, with an equimolar amount of $AgBF_4$ again yields discrete metallacyclic dications in which one bis(pyrazolyl)methane unit on each ligand remains unbound: $[Ag_2(\mu\text{-}\mathbf{L}^3)_2](BF_4)_2$ (**5**). Treatment of $\mathbf{L}^3$ with an excess of $AgBF_4$ affords a polymer of metallacycles, $\{[Ag_3(\mu\text{-}\mathbf{L}^3)_2](BF_4)_3\}_\infty$ (**6**), with one of the bis(pyrazolyl)methane units on each ligand bound to a silver cation bridging two metallacycles. The supramolecular structures of the silver(I) complexes **1**–**6** are organized by noncovalent interactions, including weak hydrogen bonding, π–π, and anion–π interactions.

Introduction

Coordination compounds of silver(I) are frequently the subject of studies that aim to design molecular and supramolecular architectures with chemical and biological applications, such as molecular recognition and catalysis.[1,2] The range of stable coordination numbers and geometries adopted by the silver(I) cation makes it possible to test a wide variety of ligand systems,[3] and the various factors that dictate the final molecular and supramolecular structures have been investigated in detail by several researchers.[4] To expand upon this body of knowledge using unique ligand systems, we are actively exploring the coordination chemistry of poly(pyrazolyl)methane compounds.[5] Modification of the substituents on the pyrazolyl rings of the original poly(pyrazolyl)methane ligands reported by Trofimenko[6] has led to a rich coordination chemistry of the resulting "second-generation" ligands.[7] We have also been interested in the possibilities afforded by functionalization at the carbon "backbone" to which each pyrazolyl ring is attached. These poly(pyrazolyl)methane compounds have been designated as "third-generation" ligands.[8] Many of our third-generation ligands are

* To whom correspondence should be addressed. E-mail: reger@mail.chem.sc.edu.

(1) For recent examples, see: (a) Seidel, R. S.; Stang, P. J. *Acc. Chem. Res.* **2002**, *35*, 972. (b) Fujita, M. *Chem. Soc. Rev.* **1998**, *27*, 417. (c) Caulder, D. L.; Raymond, K. N. *Acc. Chem. Res.* **1999**, *32*, 975. (d) Holliday, B. J.; Mirkin, C. A. *Angew. Chem., Int. Ed.* **2001**, *40*, 2022. (e) Winpenny, R. E. P. *J. Chem. Soc., Dalton Trans.* **2002**, 1. (f) Yoshizawa, M.; Takeyama, Y.; Okana, T.; Fujita, M. *J. Am. Chem. Soc.* **2003**, *125*, 3243. (g) Kusukawa, T.; Fujita, M. *J. Am. Chem. Soc.* **2002**, *124*, 13576. (h) Reger, D. L.; Semeniuc, R. F.; Smith, M. D. *Inorg. Chem.* **2003**, *42*, 8137 and references therein.

(2) (a) Lehn, J.-M. *Supramolecular Chemistry: Concepts and Perspectives*; VCH: Weinheim, 1995. (b) Steed, J. W.; Atwood, J. L. *Supramolecular Chemistry*; John Wiley: New York, 2001.

(3) (a) Khlobystov, A. N.; Blake, A. J.; Champness, N. R.; Lemenovskii, D. A.; Majouga, A. G.; Zyk, N. V.; Schröder, M. *Coord. Chem. Rev.* **2001**, *222*, 155. (b) Cortez, S. M.; Raptis, R. G. *Coord. Chem. Rev.* **1998**, *169*, 363.

(4) See, for example: (a) Piguet, C.; Bernardinelli, G.; Hopfgartner, G. *Chem. Rev.* **1997**, *97*, 2005. (b) Blake, A. J.; Champness, N. R.; Hubberstey, P.; Li, W. S.; Withersby, M. A.; Schroder, M. *Coord. Chem. Rev.* **1999**, *183*, 117. (c) Batten, S. T.; Robson, R. *Angew. Chem., Int. Ed. Engl.* **1998**, *37*, 1461. (d) Leininger, S.; Olenyuk, B.; Stang, P. J. *Chem. Rev.* **2000**, *100*, 853. (e) Seidel, R. S.; Stang, P. J. *Acc. Chem. Res.* **2002**, *35*, 972. (f) Sweigers, G. F.; Malefetse, T. J. *Chem. Rev.* **2000**, *100*, 3483. (g) Zaworotko, M. J. *Chem. Commun.* **2001**, 1. (h) Dong, Y.-B.; Cheng, J.-Y.; Huang, R.-Q.; Smith, M. D.; zur Loye, H.-C. *Inorg. Chem.* **2003**, *42*, 5699. (i) Albrecht, M. *Chem. Rev.* **2001**, *101*, 3457. (j) Reger, D. L.; Semeniuc, R. F.; Rassolov, V.; Smith, M. D. *Inorg. Chem.* **2004**, *43*, 537 and references therein. (k) Lin, R.; Yip, J. H. K. *Inorg. Chem.* **2006**, *45*, 4423.

10.1021/ic0613053 CCC: $33.50
Published on Web 10/17/2006

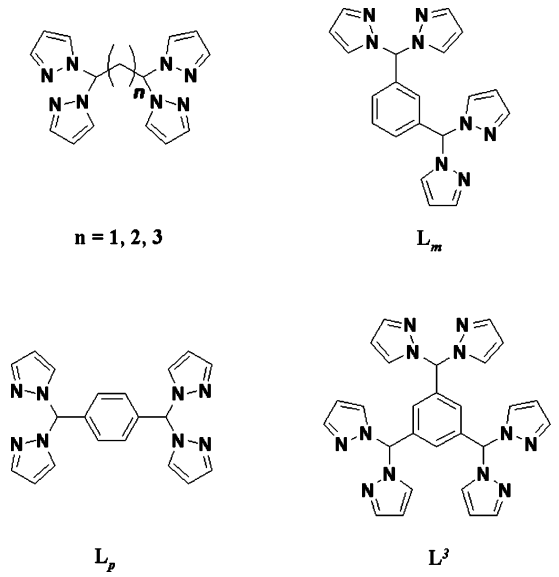

Figure 1. Alkylidene-linked[5a,b] (upper left) and arene-linked[5c,d] third-generation bis(pyrazolyl)methane ligands.

polytopic in that two or more poly(pyrazolyl)methane units are linked through the carbon backbone by organic spacers of varying flexibilities and geometries, providing multiple ligating sites.

Recently, we described a series of bitopic bis(pyrazolyl)-methane ligands linked by alkylidene spacers, $[CH(pz)_2]_2$-$(CH_2)_n$ (pz = 1-pyrazolyl; $n = 1-3$; Figure 1).[5a,b] Using the coordinatively flexible silver(I) cation, we showed how these ligands, regardless of spacer size, consistently direct the formation of discrete metallacyclic dimers of the type illustrated in Figure 2 (top) when weakly coordinating anions are used (BF_4^-, $SO_3CF_3^-$). The more strongly coordinating NO_3^-, however, shifts the preferred molecular arrangement from discrete cyclic structures to acyclic species, particularly infinite one-dimensional coordination polymers (Figure 2, bottom). In addition to building predictable molecular structures, another feature designed into these pyrazolyl-based ligands is the potential for organization of complex supramolecular structures through $\pi-\pi$ and weak hydrogen-bonding (including $CH-\pi$) interactions[9] involving the pyrazolyl groups as well as the counterions.

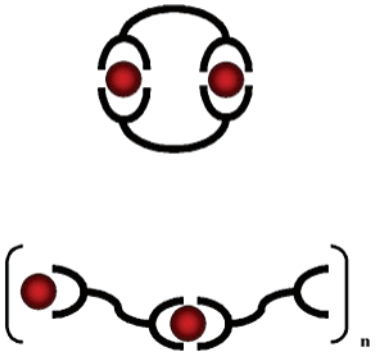

Figure 2. Representations of metallacyclic dimers (top) and infinite coordination polymers (bottom).[5a] Red spheres are metal cations. Black lines represent ligand molecules.

In general, more flexible ligands, such as the ethylene- and propylene-linked compounds in Figure 1, provide limited control over the molecular structures formed by the self-assembly process. Tectons containing rigid components, on the other hand, often restrict the types of products formed.[2] We were interested in whether replacing the flexible alkylidene linkers with arene spacers in our bis(pyrazolyl)methane compounds would allow for the formation of similar dimeric metallacycles while providing greater predictive power over the resulting molecular and supramolecular architectures. The advantage of using arene-linked ligands is that the distance between bis(pyrazolyl)methane ligating sites is fixed, unlike in the ethylene- and propylene-linked ligands, and this feature adds rigidity to the overall system. Herein, we describe the preparation and structural characterization of silver(I) complexes of the arene-linked bis(pyrazolyl)methane ligands *m*-$[CH(pz)_2]_2C_6H_4$ ($\mathbf{L}_m$),[5c] *p*-$[CH(pz)_2]_2C_6H_4$ ($\mathbf{L}_p$),[5c] and 1,3,5-$[CH(pz)_2]_3C_6H_3$ ($\mathbf{L}^3$)[5d] (Figure 1).

Experimental Section

General Considerations. Air-sensitive materials were handled under a nitrogen atmosphere using standard Schlenk techniques or in a Vacuum Atmospheres HE-493 drybox. All solvents were dried

(5) (a) Reger, D. L.; Watson, R. P.; Gardinier, J. R.; Smith, M. D. *Inorg. Chem.* **2004**, *43*, 6609. (b) Reger, D. L.; Gardinier, J. R.; Semeniuc, R. F.; Smith, M. D. *J. Chem. Soc., Dalton Trans.* **2003**, 1712. (c) Reger, D. L.; Watson, R. P.; Smith, M. D.; Pellechia, P. J. *Organometallics* **2005**, *24*, 1544. (d) Reger, D. L.; Watson, R. P.; Smith, M. D.; Pellechia, P. J. *Organometallics* **2006**, *25*, 743. (e) Reger, D. L.; Gardinier, J. R.; Grattan, T. C.; Smith, M. R.; Smith, M. D. *New J. Chem.* **2003**, *27*, 1670. (f) Reger, D. L.; Semeniuc, R. F.; Smith, M. D. *J. Organomet. Chem.* **2003**, *666*, 87. (g) Reger, D. L.; Brown, K. J.; Smith, M. D. *J. Organomet. Chem.* **2002**, *658*, 50. (h) Reger, D. L.; Wright, T. D.; Semeniuc, R. F.; Grattan, T. C.; Smith, M. D. *Inorg. Chem.* **2001**, *40*, 6212. (i) Reger, D. L.; Brown, K. J.; Gardinier, J. R.; Smith, M. D. *Organometallics* **2003**, *22*, 4973. (j) Reger, D. L.; Gardinier, J. R.; Smith, M. D. *Polyhedron* **2004**, *23*, 291.

(6) (a) Trofimenko, S. *Scorpionates: The Coordination Chemistry of Polypyrazolylborate Ligands*; Imperial College: London, 1999. (b) Trofimenko, S. *Chem. Rev.* **1993**, *93*, 943. (c) Pettinari, C.; Santini, C. *Comprehensive Coordination Chemistry II*; McCleverty, J. A., Meyer, T. J., Eds.; Elsevier: Oxford, 2004; Vol. 1, p 159. (d) Reger, D. L. *Comments Inorg. Chem.* **1999**, *21*, 1. (d) Bigmore, H. R.; Lawrence, S. C.; Mountford, P.; Tredget, C. S. *Dalton Trans.* **2005**, 635. (e) Buyers, P. K.; Canty, A. J.; Honeyman, R. T. *Adv. Organomet. Chem.* **1992**, *34*, 1. (f) Long, G. J.; Grandjean, F.; Reger, D. L. *Top. Curr. Chem.* **2004**, *233*, 91.

(7) (a) Pettinari, C.; Pettinari, R. *Coord. Chem. Rev.* **2005**, *249*, 525. (b) Pettinari, C.; Pettinari, R. *Coord. Chem. Rev.* **2005**, *249*, 663. (c) Reger, D. L.; Grattan, T. C.; Brown, K. J.; Little, C. A.; Lamba, J. J. S.; Rheingold, A. L.; Sommer, R. D. *J. Organomet. Chem.* **2000**, *607*, 120. (d) Julia, S.; del Mazo, J. M.; Avila, L.; Elguero, J. *Org. Prep. Proc. Int.* **1984**, *16*, 299.

(8) (a) Reger, D. L.; Gardinier, J. R.; Gemmill, W. R.; Smith, M. D.; Shahin, A. M.; Long, G. J.; Rebbouh, L.; Grandjean, F. *J. Am. Chem. Soc.* **2005**, *127*, 2303. (b) Reger, D. L.; Gardinier, J. R.; Bakbak, S.; Semeniuc, R. F.; Bunz, U. H. F.; Smith, M. D. *New J. Chem.* **2005**, *29*, 1035. (c) White, D.; Faller, J. W. *J. Am. Chem. Soc.* **1982**, *104*, 1548. (d) Brock, C. P.; Das, M. K.; Minton, R. P.; Niedenzu, K. *J. Am. Chem. Soc.* **1988**, *110*, 817. (e) Janiak, C.; Braun, L.; Girgsdies, F. *J. Chem. Soc., Dalton Trans.* **1999**, 3133. (f) Kisko, J. L.; Hascall, T.; Kimblin, C.; Parkin, G. *J. Chem. Soc., Dalton Trans.* **1999**, 1929. (g) Hardin, N. C.; Jeffrey, J. C.; McCleverty, J. A.; Rees, L. H.; Ward, M. A. *New J. Chem.* **1998**, *22*, 661. (h) Niedenzu, K.; Trofimenko, S. *Inorg. Chem.* **1985**, *24*, 4222. (i) Jäkle, F.; Polborn, K.; Wagner, M. *Chem. Ber.* **1996**, *129*, 603. (j) Fabrizi de Biani, F.; Jäkle, F.; Spiegler, M.; Wagner, M.; Zanello, P. *Inorg. Chem.* **1997**, *36*, 2103. (k) Herdtweck, E.; Peters, F.; Scherer, W.; Wagner, M. *Polyhedron* **1998**, *17*, 1149. (l) Guo, S. L.; Peters, F.; Fabrizi de Biani, F.; Bats, J. W.; Herdtweck, E.; Zanello, P.; Wagner, M. *Inorg. Chem.* **2001**, *40*, 4928. (m) Guo, S. L.; Bats, J. W.; Bolte, M.; Wagner, M. *J. Chem. Soc., Dalton Trans.* **2001**, 3572. (n) Bieller, S.; Zhang, F.; Bolte, M.; Bats, J. W.; Lerner, H.-W.; Wagner, M. *Organometallics* **2004**, *23*, 2107.

by conventional methods prior to use. The compounds *m*-[CH(pz)$_2$]$_2$C$_6$H$_4$,[5c] *p*-[CH(pz)$_2$]$_2$C$_6$H$_4$,[5c] and 1,3,5-[CH(pz)$_2$]$_3$C$_6$H$_3$[5d] were prepared following reported procedures. All other chemicals were purchased from Aldrich or Fisher Scientific and used as received. Reported melting points are uncorrected. IR spectra were obtained on a Nicolet 5DXBO FTIR spectrometer. NMR spectra were recorded on a Varian Mercury/VX 300 or 400 spectrometer. All chemical shifts are in ppm. ^{1}H NMR spectra were secondary referenced using the signals from residual undeuterated solvents. ^{19}F NMR spectra were externally referenced to $CFCl_3$. Mass spectrometric measurements were obtained on a MicroMass QTOF spectrometer. Elemental analyses were performed on vacuum-dried samples by Robertson Microlit Laboratories (Madison, NJ).

Syntheses of Silver Complexes. Silver complexes **1**−**4** were prepared by the following general procedure: To a foil-covered, 10-mL THF solution of $AgBF_4$ (0.070 g, 0.36 mmol) or $AgPF_6$ (0.080 g, 0.32 mmol) was added by cannula an equimolar, 15-mL THF solution of *m*-C$_6$H$_4$[CH(pz)$_2$]$_2$ (**L**$_m$) or *p*-C$_6$H$_4$[CH(pz)$_2$]$_2$ (**L**$_p$). A white precipitate immediately formed. After stirring in the dark for 3−5 h, the solvent was removed in vacuo and the remaining white solid was washed with 5 mL of THF and dried in vacuo overnight. Crystals for elemental analyses, grown by vapor diffusion of Et_2O into 1-mL CH_3CN (acetone for **1**) solutions of the solids, were isolated by filtration, rinsed with Et_2O, and dried in vacuo. X-ray-quality crystals were grown in the same manner and taken directly from the mother liquor.

The silver complexes **5** and **6** were prepared by dissolving a mixture of 1,3,5-[CH(pz)$_2$]$_3$C$_6$H$_3$ (**L**^{3}, 0.050 g, 0.097 mmol) and $AgBF_4$ (0.019 g, 0.098 mmol for **5**; 0.057 g, 0.29 mmol for **6**) in a minimum amount of CH_3CN and allowing Et_2O to diffuse into 1-mL portions of the resulting solutions. Crystals formed within 2 days. Crystals for X-ray analysis were taken directly from the mother liquor. All other crystals for characterization were isolated by filtration, rinsed with Et_2O, and dried in vacuo.

[Ag$_2$(*μ*-*m*-[CH(pz)$_2$]$_2$C$_6$H$_4$)$_2$](BF$_4$)$_2$ (1). Yield = 0.15 g (65%). Mp > 300 °C. Anal. Calcd for $C_{40}H_{36}Ag_2B_2F_8N_{16}$: C, 42.51; H, 3.21; N, 19.83. Found: C, 42.56; H, 2.99; N, 19.77. IR (KBr, cm^{-1}): 3150, 3134, 2987, 1520, 1454, 1070, 825, 760, 519. ^{1}H NMR (400 MHz, CD_3CN): δ 7.81 (dd, J = 0.6, 2.6 Hz, 4 H, 5/3-pz), 7.80 (s, 2 H, C*H*(pz)$_2$), 7.55 (d, J = 2.0 Hz, 4 H, 5/3-pz), 7.40 (t, J = 7.8 Hz, 1 H, C$_6$*H*$_4$), 6.89 (d, J = 7.6 Hz, 2 H, C$_6$*H*$_4$), 6.37 (t, J = 2.2 Hz, 4 H, 4-pz), 6.23 (s, 1 H, C$_6$*H*$_4$). ^{19}F NMR (376 MHz, CD_3CN): δ −152. MS ESI(+) *m*/*z* (rel. % abund.) [assgn]: 1043 (10) [Ag$_2$(**L**$_m$)$_2$BF$_4$]$^+$, 847 (30) [Ag(**L**$_m$)$_2$]$^+$, 479 (100) [Ag**L**$_m$]$^+$, 371 (65) [H**L**$_m$]$^+$, 303 (80) [**L**$_m$ − pz]$^+$.

[Ag$_2$(*μ*-*m*-[CH(pz)$_2$]$_2$C$_6$H$_4$)$_2$](PF$_6$)$_2$ (2). Yield = 0.15 g (76%). Mp > 300 °C. Anal. Calcd for $C_{40}H_{36}Ag_2F_{12}N_{16}P_2$: C, 38.54; H, 2.91; N, 17.98. Found: C, 38.83; H, 2.68; N, 18.32. IR (KBr, cm^{-1}): 3150, 3134, 1520, 1446, 1401, 1295, 1103, 837, 760, 555. ^{1}H NMR (400 MHz, CD_3CN): δ 7.79 (s, 2 H, C*H*(pz)$_2$) 7.75 (d, J = 2.0 Hz, 4 H, 5/3-pz), 7.54 (d, J = 1.6 Hz, 4 H, 5/3-pz), 7.40 (t, J = 7.8 Hz, 1 H, C$_6$*H*$_4$), 6.94 (dd, J = 2.0, 7.6 Hz, 2 H, C$_6$*H*$_4$), 6.38 (br s, 1 H, C$_6$*H*$_4$) 6.35 (t, J = 2.2 Hz, 4 H, 4-pz). ^{19}F NMR (376 MHz, CD_3CN): δ −73 (d, J_{F-P} = 706 Hz). MS ESI(+) *m*/*z* (rel. % abund.) [assgn]: 1101 (20) [Ag$_2$(**L**$_m$)$_2$PF$_6$]$^+$, 847 (30) [Ag(**L**$_m$)$_2$]$^+$, 479 (100) [Ag**L**$_m$]$^+$, 371 (50) [H**L**$_m$]$^+$, 303 (60) [**L**$_m$ − pz]$^+$.

{**[Ag(*μ*-*p*-[CH(pz)$_2$]$_2$C$_6$H$_4$)]BF$_4$**}$_\infty$ **(3).** Yield = 0.19 g (95%). Mp > 300 °C. Anal. Calcd for $C_{20}H_{18}AgBF_4N_8$: C, 42.51; H, 3.21; N, 19.83. Found: C, 42.50; H, 2.94; N, 20.07. IR (KBr, cm^{-1}): 3126, 3109, 1516, 1446, 1401, 1287, 1099, 1050, 796, 764. ^{1}H NMR (400 MHz, CD_3CN): δ 7.82 (s, 2 H, C*H*(pz)$_2$), 7.79 (d, J = 2.4 Hz, 4 H, 5/3-pz), 7.55 (d, J = 1.6 Hz, 4 H, 5/3-pz), 6.87 (s, 4 H, C$_6$*H*$_4$), 6.38 (t, J = 2.2 Hz, 4 H, 4-pz).^{19}F NMR (376 MHz, CD_3CN): δ −152. MS ESI(+) *m*/*z* (rel. % abund.) [assgn]: 847 (35) [Ag(**L**$_p$)$_2$]$^+$, 477 (50) [Ag**L**$_p$]$^+$, 371 (45) [H**L**$_p$]$^+$, 303 (100) [**L**$_p$ − pz]$^+$.

{**[Ag(*μ*-*p*-[CH(pz)$_2$]$_2$C$_6$H$_4$)]PF$_6$**}$_\infty$ **(4).** Yield = 0.16 g (82%). Mp > 300 °C. Anal. Calcd for $C_{21}H_{19.5}AgF_6N_{8.5}P$ (**4**·0.5CH_3CN): C, 39.18; H, 3.06; N, 18.49. Found: C, 39.17; H, 2.71; N, 18.43. IR (KBr, cm^{-1}): 3146, 1446, 1397, 1295, 1095, 1050, 845, 760, 559. ^{1}H NMR (400 MHz, CD_3CN): δ 7.82 (s, 2 H, C*H*(pz)$_2$), 7.78 (d, J = 2.0 Hz, 4 H, 5/3-pz), 7.56 (d, J = 1.2 Hz, 4 H, 5/3-pz), 6.89 (s, 4 H, C$_6$*H*$_4$), 6.38 (t, J = 2.2 Hz, 4 H, 4-pz).^{19}F NMR (376 MHz, CD_3CN): δ −73 (d, J_{F-P} = 706 Hz). MS ESI(+) *m*/*z* (rel. % abund.) [assgn]: 847 (40) [Ag(**L**$_p$)$_2$]$^+$, 477 (80) [Ag**L**$_p$]$^+$, 371 (50) [H**L**$_p$]$^+$, 303 (100) [**L**$_p$ − pz]$^+$.

[Ag$_2$(*μ*-1,3,5-[CH(pz)$_2$]$_3$C$_6$H$_3$)$_2$](BF$_4$)$_2$ (5). Yield = 0.040 g (58%). Mp > 300 °C. Anal. Calcd for $C_{54}H_{48}Ag_2B_2F_8N_{24}$: C, 45.59; H, 3.40; N, 23.63. Found: C, 45.43; H, 3.49; N, 23.35. IR (KBr, cm^{-1}): 3142, 3121, 3109, 3011, 2983, 1520, 1462, 1442, 1393, 1058, 784, 756, 523.^{1}H NMR (300 MHz, CD_3CN): δ 7.75 (s, 3 H, C*H*(pz)$_2$), 7.68 (dd, J = 0.6, 2.7 Hz, 6 H, 5/3-pz), 7.50 (d, J = 1.5 Hz, 6 H, 5/3-pz), 6.46 (d, J = 0.6 Hz, 3 H, C$_6$*H*$_3$), 6.32 (dd, J = 1.8, 2.4 Hz, 6 H, 4-pz). ^{19}F NMR (376 MHz, CD_3CN): δ −152. MS ESI(+) *m*/*z* (rel. % abund.) [assgn]: 1335 (1) [Ag$_2$(**L**^{3})$_2$(BF$_4$)]$^+$, 1139 (20) [Ag(**L**^{3})$_2$]$^+$, 625 (100) [Ag**L**^{3}]$^+$, 517 (55) [H**L**^{3}]$^+$, 449 (40) [**L**^{3} − pz]$^+$. HRMS: ESI(+) (*m*/*z*) calcd for $C_{54}H_{48}Ag_2BF_4N_{24}$, [Ag$_2$(**L**^{3})$_2$(BF$_4$)]$^+$ 1335.2635, found 1335.2595.

{**[Ag$_3$(*μ*-1,3,5-[CH(pz)$_2$]$_3$C$_6$H$_3$)$_2$](BF$_4$)$_3$**}$_\infty$ **(6).** Yield = 0.070 g (89%). Mp > 300 °C. Anal. Calcd for $C_{54}H_{48}Ag_3B_3F_{12}N_{24}$: C, 40.11; H, 2.99; N, 20.79. Found: C, 40.33; H, 3.03; N, 21.11. IR (KBr, cm^{-1}): 3126, 2974, 1524, 1401, 1303, 1074, 788, 768, 514.^{1}H NMR (300 MHz, CD_3CN): δ 7.74 (s, 3 H, C*H*(pz)$_2$), 7.71 (dd, J = 0.6, 2.7 Hz, 6 H, 5/3-pz), 7.49 (dd, J = 0.6, 2.1 Hz, 6 H, 5/3-pz), 6.39 (s, 3 H, C$_6$*H*$_3$), 6.32 (dd, J = 1.8, 2.4 Hz, 6 H, 4-pz). ^{19}F NMR (376 MHz, CD_3CN): δ −152. MS ESI(+) *m*/*z* (rel. % abund.) [assgn]: 1531 (1) [Ag$_3$(**L**^{3})$_2$(BF$_4$)$_2$]$^+$, 1335 (10) [Ag$_2$(**L**^{3})$_2$-(BF$_4$)]$^+$, 1139 (10) [Ag(**L**^{3})$_2$]$^+$, 625 (100) [Ag**L**^{3}]$^+$, 517 (15) [H**L**^{3}]$^+$, 449 (15) [**L**^{3} − pz]$^+$.

Crystal Structure Determinations. X-ray intensity data from a colorless hexagonal, rod-shaped crystal of **1**·2$(CH_3)_2CO$·0.43H_2O, a colorless plate of **2**, a colorless bar-shaped crystal of **3**, a colorless needle of **4**·0.5CH_3CN, and colorless prisms of **5** and **6**·2CH_3CN were measured at 150(1) K (200(1) K for **3**) on a Bruker SMART APEX CCD-based diffractometer (Mo Kα radiation, λ = 0.71073 Å).[10] Raw data frame integration and Lp corrections were performed with SAINT+.[10] Final unit cell parameters were determined by least-squares refinement of 2905, 5652, 4331, 7064, 7531, and 8971 strong reflections for **1**−**6**, respectively. Analyses of the data showed negligible crystal decay during data collection. Direct methods structure solution, difference Fourier calculations, and full-matrix least-squares refinement against F^2 were performed with SHELXTL.[11] All non-hydrogen atoms were refined with anisotropic displacement parameters except where noted. Hydrogen atoms were placed in geometrically idealized positions and included as riding atoms. Details of the data collections are given in Table 1, while

(9) For examples, see: (a) Desiraju, G. R. *Acc. Chem. Res.* **2002**, *35*, 565. (b) Steiner, T. *Angew. Chem., Int. Ed.* **2002**, *41*, 48. (c) Cited papers in reference in 4j. (d) Rowland, R. S.; Taylor, R. *J. Phys. Chem.* **1996**, *100*, 7384.

(10) *SMART*, Version 5.630; Bruker Analytical X-ray Systems, Inc.: Madison, WI, 2003. *SAINT+*, Version 6.45; Bruker Analytical X-ray Systems, Inc.: Madison, WI, 2003.

(11) Sheldrick, G. M. *SHELXTL*, Version 6.1; Bruker Analytical X-ray Systems, Inc.: Madison, WI, 2000.

Table 1. Crystal Data and Refinement Details for $[Ag_2(\mu\text{-}m\text{-}[CH(pz)_2]_2C_6H_4)_2](BF_4)_2\cdot 2(CH_3)_2CO\cdot 0.43H_2O$ (**1**·$2(CH_3)_2CO\cdot 0.43H_2O$), $[Ag_2(\mu\text{-}m\text{-}[CH(pz)_2]_2C_6H_4)_2](PF_6)_2$ (**2**), $\{[Ag(\mu\text{-}p\text{-}[CH(pz)_2]_2C_6H_4)]BF_4\}_\infty$ (**3**), $\{[Ag(\mu\text{-}p\text{-}[CH(pz)_2]_2C_6H_4)_2]PF_6\cdot 0.5CH_3CN\}_\infty$ (**4**·$0.5CH_3CN$), $[Ag_2(\mu\text{-}1,3,5\text{-}[CH(pz)_2]_3C_6H_3)_2](BF_4)_2$ (**5**), and $[Ag_3(\mu\text{-}1,3,5\text{-}[CH(pz)_2]_3C_6H_3)_2](BF_4)_3\cdot 2CH_3CN$ (**6**·$2CH_3CN$)

	1·$2(CH_3)_2CO\cdot 0.43H_2O$	**2**	**3**	**4**·$0.5CH_3CN$	**5**	**6**·$2CH_3CN$
empirical formula	$C_{46}H_{48.85}Ag_2B_2F_8N_{16}O_{2.43}$	$C_{40}H_{36}Ag_2F_{12}N_{16}P_2$	$C_{20}H_{18}AgBF_4N_8$	$C_{21}H_{19.50}AgF_6N_{8.50}P$	$C_{54}H_{48}Ag_2B_2F_8N_{24}$	$C_{58}H_{54}Ag_3B_3F_{12}N_{26}$
fw	1254.05	1246.53	565.10	643.79	1422.52	1699.31
T (K)	150(1)	150(1)	200(1)	150(1)	150(1)	150(1)
cryst syst	trigonal	monoclinic	triclinic	monoclinic	orthorhombic	triclinic
space group	$R\bar{3}$	$P2_1/c$	$P\bar{1}$	$P2_1/n$	$Pbca$	$P\bar{1}$
a, Å	31.1829(7)	10.4689(5)	9.1941(4)	19.4787(9)	16.3200(8)	12.2901(6)
b, Å	31.1829(7)	13.7249(6)	11.7500(5)	11.9258(6)	16.8460(8)	14.7478(7)
c, Å	14.4581(7)	16.8065(8)	11.8114(5)	21.3614(10)	21.6388(10)	20.6296(10)
α, deg	90	90	60.5720(10)	90	90	70.6900(10)
β, deg	90	102.5020(10)	85.6080(10)	96.6930(10)	90	83.0950(10)
γ, deg	120	90	86.0190(10)	90	90	85.5340(10)
V, Å^3	12175.2(7)	2357.58(19)	1107.35(8)	4928.4(4)	5949.1(5)	3500.3(3)
Z	9	2	2	8	4	2
D (calcd), Mg·m^{-3}	1.539	1.756	1.695	1.735	1.588	1.612
abs coeff, mm^{-1}	0.806	0.997	0.970	0.958	0.744	0.922
cryst size, mm^3	0.46 × 0.16 × 0.10	0.18 × 0.12 × 0.04	0.20 × 0.12 × 0.08	0.46 × 0.14 × 0.10	0.34 × 0.22 × 0.14	0.44 × 0.38 × 0.35
final R indices [$I > 2\sigma(I)$]						
R1	0.0448	0.0448	0.0392	0.0346	0.0407	0.0308
wR2	0.1009	0.0757	0.0962	0.0757	0.1043	0.0863

further notes regarding the solution and refinement for all six structures follow.

The compound **1**·$2(CH_3)_2CO\cdot 0.43H_2O$ crystallizes in the trigonal/rhombohedral crystal system. The pattern of systematic absences in the intensity data positively ruled out a *c*-glide symmetry operation; the space group $R\bar{3}$ was eventually confirmed by the successful solution and refinement of the data. The asymmetric unit consists of one-half of a $[Ag_2(\mu\text{-}m\text{-}[CH(pz)_2]_2C_6H_4)_2]^{2+}$ cation located on an inversion center, one BF_4^- anion, an acetone molecule of crystallization, and two partially occupied water molecule sites. Thorough understanding of the full crystal structure and composition is hampered by disorder. The acetone molecule is disordered over two orientations. Occupancies were initially refined and subsequently fixed near the final refined values. These atoms were assigned a common isotropic displacement parameter. There are two isolated electron density peaks which were modeled as water molecules O3S and O4S. These two atoms were given a fixed isotropic displacement parameter and their occupancies refined. No hydrogen atoms were located or refined for these atoms. Elongated displacement ellipsoids of the fluorine atoms of the BF_4^- anion indicate mild disorder of this group, which was not modeled. The large average displacement parameters for the BF_4^- anion and for the disordered species and the presence of several residual electron density peaks in the disorder regions indicate the limitations of the model employed.

Compound **2** crystallizes in the space group $P2_1/c$ as determined uniquely by the pattern of systematic absences in the intensity data. The asymmetric unit contains one-half of a discrete $[Ag_2(\mu\text{-}m\text{-}[CH(pz)_2]_2C_6H_4)_2]^{2+}$ cation located on an inversion center and one PF_6^- anion.

Compound **3** crystallizes in the triclinic system. The space group $P\bar{1}$ was confirmed by the successful solution and refinement of the structure. The asymmetric unit consists of one Ag atom, one-half each of two independent *p*-$[CH(pz)_2]_2C_6H_4$ ligands, both located on inversion centers, and a disordered BF_4^- anion. A reasonable and stable disorder model involving three components was refined for the anion. Occupancies of the three components were refined but constrained to sum to unity. A total of 31 distance restraints were used to maintain chemically reasonable B−F and F−F distances. All non-hydrogen atoms were refined with anisotropic displacement parameters except the anion atoms (isotropic).

The compound **4**·$0.5CH_3CN$ crystallizes in the space group $P2_1/n$ as determined uniquely by the pattern of systematic absences in the intensity data. The asymmetric unit contains two Ag centers, one complete *p*-$[CH(pz)_2]_2C_6H_4$ ligand and one-half each of two additional *p*-$[CH(pz)_2]_2C_6H_4$ ligands (both on inversion centers), two independent PF_6^- anions, and one acetonitrile molecule of crystallization.

Compound **5** crystallizes in the orthorhombic space group *Pbca* as determined uniquely by the pattern of systematic absences in the intensity data. The asymmetric unit contains one Ag center, one ligand, and one BF_4^- counterion.

The compound **6**·$2CH_3CN$ crystallizes in the triclinic system. The space group $P\bar{1}$ was confirmed by the successful solution and refinement of the data. The asymmetric unit contains three Ag centers, three BF_4^- counterions, two complete 1,3,5-$[CH(pz)_2]_3C_6H_3$ ligands, two identifiable acetonitrile molecules of crystallization, and a region of disordered solvent which could not be modeled successfully. The contribution of the solvent was removed from the structure factor calculations with the Squeeze program in PLATON (165.1 Å^3 solvent-accessible void volume centered at 0, 1/2, 1/2; 38 e$^-$/cell).[12] The final tabulated fw, d(calcd), and F(000) do not include the unknown solvent species.

Results

Syntheses and Characterization. Combining separate THF solutions of AgX (X = BF_4^-, PF_6^-) and *m*-$[CH(pz)_2]_2C_6H_4$ (**L**$_m$) resulted in the precipitation of complexes $[Ag_2(\mu\text{-}m\text{-}[CH(pz)_2]_2C_6H_4)_2](BF_4)_2$ (**1**) and $[Ag_2(\mu\text{-}m\text{-}[CH(pz)_2]_2C_6H_4)_2](PF_6)_2$ (**2**) according to eq 1. Similarly, combination of THF solutions of AgX and *p*-$[CH(pz)_2]_2C_6H_4$ (**L**$_p$) gave white precipitates of the complexes $\{Ag(\mu\text{-}p\text{-}[CH(pz)_2]_2C_6H_4)]BF_4\}_\infty$ (**3**) and $\{[Ag(\mu\text{-}p\text{-}[CH(pz)_2]_2C_6H_4)]PF_6\}_\infty$ (**4**) as given in eq 2. Elemental analyses of **1**−**4** were consistent with the empirical formulas [AgL]X (L = **L**$_m$ or **L**$_p$; X = BF_4^- or PF_6^-). X-ray crystallographic analyses, discussed below, confirmed that complexes of **L**$_m$ (**1** and **2**) exist as discrete metallacyclic dimers and that complexes of **L**$_p$ (**3** and **4**), in contrast, form simple (acyclic) coordination polymers.

(12) PLATON/PLUTON: (a) Spek, A. L. *Acta Crystallogr., Sect. A* **1990**, *46*, C34. (b) Spek, A. L. *PLATON, A Multipurpose Crystallographic Tool*; Utrecht University: Utrecht, The Netherlands, 1998.

$$2AgX + 2\mathbf{L}_m \rightarrow [Ag_2(\mu\text{-}\mathbf{L}_m)_2]X_2,\ X = BF_4^-\ (\mathbf{1}),\ PF_6^-\ (\mathbf{2}) \quad (1)$$

$$AgX + \mathbf{L}_p \rightarrow \{[Ag(\mu\text{-}\mathbf{L}_p)]X\}_\infty,\ X = BF_4^-\ (\mathbf{3}),\ PF_6^-\ (\mathbf{4}) \quad (2)$$

Dissolving equimolar amounts of $AgBF_4$ and 1,3,5-[$CH(pz)_2]_3C_6H_3$ ($\mathbf{L}^3$) together in acetonitrile and allowing ether to slowly diffuse into these solutions yielded crystals of [$Ag_2(\mu$-1,3,5-$[CH(pz)_2]_3C_6H_3)_2](BF_4)_2$ (**5**, eq 3). Analysis of complex **5** indicated an empirical formula [$Ag\mathbf{L}^3$]BF_4 with a one-to-one silver-to-ligand ratio. X-ray crystallographic studies of **5** confirmed the presence of discrete metallacyclic dications in which one bis(pyrazolyl)methane unit on each ligand in the metallacycle is unbound. When $\mathbf{L}^3$ and an excess of $AgBF_4$ were dissolved in acetonitrile and ether was allowed to slowly diffuse into these solutions, compound $\{[Ag_3(\mu$-1,3,5-$[CH(pz)_2]_3C_6H_3)_2](BF_4)_3\}_\infty$ (**6**) was obtained (eq 4). Analysis of **6** yielded an empirical formula corresponding to a three-to-two silver-to-ligand ratio, and crystallographic studies revealed that **6** consists of a polymer of metallacycles resulting from coordination of the third bis(pyrazolyl)methane unit on each ligand to an additional silver cation.

$$2AgBF_4 + 2\mathbf{L}^3 \rightarrow [Ag_2(\mu\text{-}\mathbf{L}^3)_2](BF_4)_2\ (\mathbf{5}) \quad (3)$$

$$3AgBF_4 + 2\mathbf{L}^3 \rightarrow \{[Ag_3(\mu\text{-}\mathbf{L}^3)_2](BF_4)_3\}_\infty\ (\mathbf{6}) \quad (4)$$

The positive-ion electrospray (ESI(+)) mass spectra of the complexes derived from $\mathbf{L}_m$, **1** and **2**, contained peaks corresponding to dimeric metallacycles associated with one counterion, $[Ag_2(\mathbf{L}_m)_2(BF_4)]^+$ or $[Ag_2(\mathbf{L}_m)_2(PF_6)]^+$. A peak corresponding to the free dication, however, was not observed for either compound. Instead, the monocation $[Ag\mathbf{L}_m]^+$, whose peak pattern is distinct from that of the free dicationic dimer, gave rise to the base peak in the spectra of both **1** and **2**. As opposed to complexes of $\mathbf{L}_m$, complexes of $\mathbf{L}_p$, **3** and **4**, showed no peaks corresponding to dimers as observed for **1** and **2**. The remaining features of the spectra of **3** and **4**, including the presence of the peak from $[Ag\mathbf{L}_p]^+$, were identical to those observed in the spectra of **1** and **2** with the exception that the base peaks for **3** and **4** were due to the species formed by loss of one pyrazolyl group from the free ligand, $[\mathbf{L}_p - pz]^+$, rather than the monocation $[Ag\mathbf{L}_p]^+$. The ESI(+) mass spectrum of **5** also showed the respective dimeric metallacycle, $[Ag_2(\mathbf{L}^3)_2(BF_4)]^+$, as well as the monocation $[Ag\mathbf{L}^3]^+$. The spectrum of **6** was identical except that it also displayed a peak resulting from association of an additional $AgBF_4$ equivalent, namely, $[Ag_3(\mathbf{L}^3)_2(BF_4)_2]^+$. Spectra of all six compounds exhibited a peak due to the silver cation bound to two ligands, $[AgL_2]^+$.

Proton NMR spectra of all six complexes in acetonitrile showed only one set of ligand signals, shifted downfield of those of the respective free ligand. Since the complexes, particularly those consisting of metallacycles, are expected to show nonequivalence of ligand protons, the silver complexes must be labile in solution and undergo ligand exchange that is rapid on the NMR time scale. This result is consistent with previously studied poly(pyrazolyl)methane complexes of silver(I).[4j,5a,b] Infrared spectra of all six compounds showed the expected B−F and P−F stretching frequencies (ca. 1070 and 777 cm^{-1} for BF_4^- and ca. 865 cm^{-1} for PF_6^-).[13]

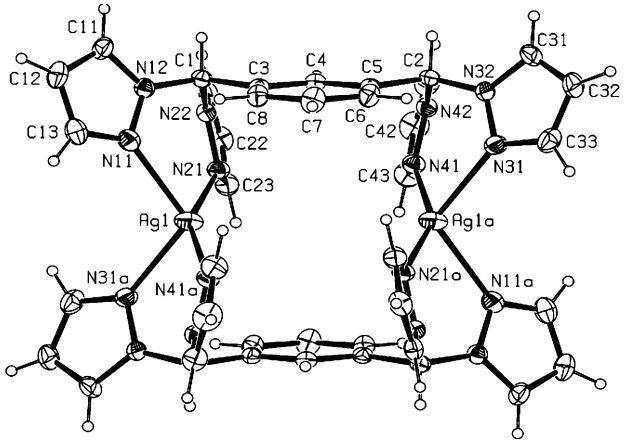

Figure 3. ORTEP drawing of the cationic unit in [$Ag_2(\mu$-*m*-$[CH(pz)_2]_2C_6H_4)_2](BF_4)_2\cdot 2(CH_3)_2CO\cdot 0.43H_2O$ (**1**·$2(CH_3)_2CO\cdot 0.43H_2O$). Displacement ellipsoids are drawn at the 30% probability level. The complex [$Ag_2(\mu$-*m*-$[CH(pz)_2]_2C_6H_4)_2](PF_6)_2$ (**2**) contains analogous cations. Selected bond distances (Å) and angles (deg) for **1**·$2(CH_3)_2CO\cdot 0.43H_2O$: Ag(1)−N(11) 2.366(4), Ag(1)−N(21) 2.247(4), Ag(1)−N(31a) 2.382(4), Ag(1)−N(41a) 2.239(4); N(11)−Ag(1)−N(21) 85.47(14), N(11)−Ag(1)−N(31a) 111.59(13), N(11)−Ag(1)−N(41a) 112.81(14), N(21)−Ag(1)−N(31a) 106.94(14), N(21)−Ag(1)−N(41a) 152.27(14), N(31a)−Ag(1)−N(41a) 86.22(14). Selected bond distances (Å) and angles (deg) for **2**: Ag(1)−N(11) 2.373(4), Ag(1)−N(21) 2.235(3), Ag(1)−N(31a) 2.238(4), Ag(1)−N(41a) 2.424(4); N(11)−Ag(1)−N(21) 84.89(13), N(11)−Ag(1)−N(31a) 111.34(12), N(11)−Ag(1)−N(41a) 102.61(12), N(21)−Ag(1)−N(31a) 158.54(13), N(21)−Ag(1)−N(41a) 106.64(12), N(31a)−Ag(1)−N(41a) 84.11(13).

Solid-State Structures. (a) Complexes of Bitopic Ligands: Metallacycles. The crystalline forms of [$Ag_2(\mu$-*m*-$[CH(pz)_2]_2C_6H_4)_2](BF_4)_2$ (**1**), which crystallizes with two molecules of acetone and trace water, and [$Ag_2(\mu$-*m*-$[CH(pz)_2]_2C_6H_4)_2](PF_6)_2$ (**2**) exist in the solid state as discrete metallacycles where two ligand molecules are each bridging two silver cations. An ORTEP representation of the dicationic macrocycle in **1**·$2(CH_3)_2CO\cdot 0.43H_2O$ is shown in Figure 3. The dication in **2** is analogous, and the cations of both **1** and **2** lie on inversion centers. The environment about the silver ions is distorted tetrahedral with the chelate ring bite imposing N−Ag−N angles of 85° and 86° for **1**·$2(CH_3)_2CO\cdot 0.43H_2O$ and 84° and 85° for **2**. Silver−nitrogen bond lengths for both complexes are typical but asymmetric with most values falling between 2.24 and 2.38 Å. Compound **2** possesses a longer Ag−N distance of 2.42 Å. The Ag···Ag distances across the argentacycles are 5.31 and 4.83 Å for **1**·$2(CH_3)_2CO\cdot 0.43H_2O$ and **2**.

The packing of the argentacycles and the BF_4^- anions in **1**·$2(CH_3)_2CO\cdot 0.43(H_2O)$ is governed by CH−F hydrogen-bonding interactions, the most prominent of which give rise to infinite one-dimensional ribbons running along the *c*-axis direction. This primary linkage involves both of the unique methine hydrogen atoms (H(1) and H(2)) and two BF_4^- anions, which are sandwiched between two argentacycles

(13) Nakamoto, K. *Infrared and Raman Spectra of Inorganic Coordination Compounds*, 4th ed.; John Wiley: New York, 1986.

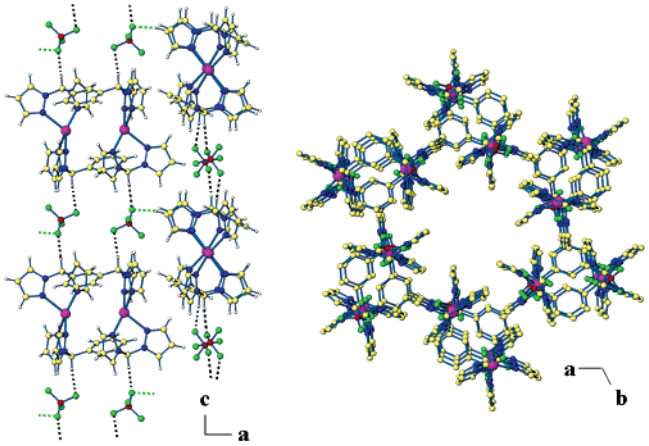

Figure 4. Illustrations of the extended structure of **1**·2$(CH_3)_2CO$·0.43H_2O. (Left) View perpendicular to two adjacent 1-D ribbons (vertical). CH−F hydrogen bonds which link the argentacycles into ribbons are shown as black dashed bonds; those which link the individual ribbons are shown in green. (Right) Perspective view down the *c*-axis direction parallel to six 1-D ribbons. Hydrogen atoms and solvent molecules are omitted, and CH−F interactions are not indicated.

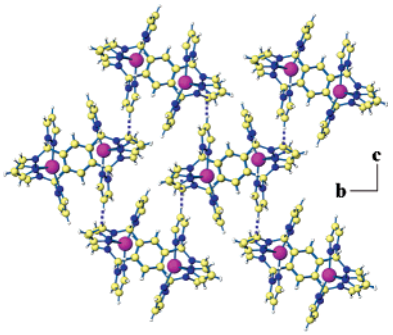

Figure 5. View of a sheet in the *bc* plane of **2** organized by CH−π interactions (purple dashed lines).

(CH−F distances 2.05 and 2.20 Å; Figure 4, left). Longer CH−F (2.4−2.5 Å) interactions between pyrazolyl ring hydrogen atoms serve to aggregate the individual ribbons into a distinct three-dimensional honeycomb structure, one "cell" of which is shown in Figure 4 (right). The cells caused by the honeycomb arrangement of argentacycles and BF_4^- ions are channels extending along the *c*-axis direction, and they contain the disordered acetone and water molecules (not pictured).

The structure of **2** is replete with significant noncovalent interactions. The supramolecular three-dimensional framework of **2** consists of parallel sheets of argentacycles in the *bc* plane that stack along the *a* axis. As shown in Figure 5, the planes of argentacycles are organized by CH−π interactions between pyrazolyl hydrogen atoms at the 4-position and pyrazolyl rings on adjacent cations (CH−centroid distance 2.70 Å; angle 165°). Each metallacycle is participating in four of these CH−π interactions with four neighboring metallacycles, and each contains two hydrogen-atom donors (the 4-pyrazolyl hydrogen atoms) and two hydrogen-atom acceptors (pyrazolyl rings). The packing of these sheets along the *a* axis is directed by $\pi-\pi$ interactions (3.64 Å; Figure 6) between ideally aligned central phenylene rings from neighboring sheets. The interacting rings are perfectly parallel, and their centroids are offset by 17°.

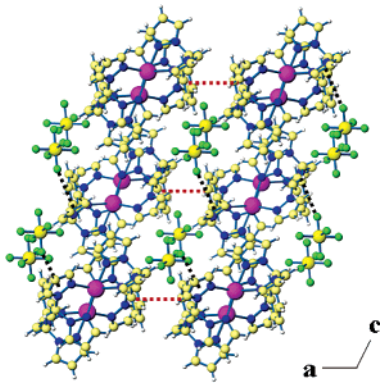

Figure 6. View down the *b* axis of **2** showing $\pi-\pi$ stacking (red dashed lines) of parallel sheets of metallacycles and embedded layers of PF_6^- anions participating in anion−π interactions (black dashed lines).

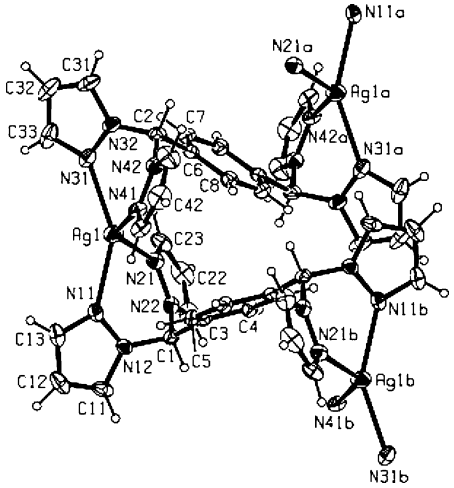

Figure 7. ORTEP drawing of the cationic coordination polymer in {[Ag(μ-*p*-$[CH(pz)_2]_2C_6H_4$)]BF_4}$_\infty$ (**3**). Displacement ellipsoids are drawn at the 30% probability level. Selected bond distances (Å) and angles (deg): Ag(1)−N(11) 2.300(3), Ag(1)−N(21) 2.339(3), Ag(1)−N(31) 2.282(3), Ag(1)−N(41) 2.391(3); N(11)−Ag(1)−N(21) 81.28(11), N(11)−Ag(1)−N(31) 148.42(12), N(11)−Ag(1)−N(41) 106.03(1), N(21)−Ag(1)−N(31) 117.15(11), N(21)−Ag(1)−N(41) 132.36(11), N(31)−Ag(1)−N(41) 81.05(11).

The PF_6^- anions in **2**, which exist in layers embedded between the sheets, take part in both CH−F and anion−π interactions that support the $\pi-\pi$ stacking shown in Figure 6 by bridging the parallel sheets of argentacycles. The CH−F bonds (not shown) are in the range of 2.2−2.5 Å and include hydrogen-atom acceptors from the pyrazolyl rings, methine hydrogen atoms on the $-CH(pz)_2$ units, and the central ligand arene ring. Only one of the two sets of anion−π interactions is illustrated in Figure 6. These interactions are long with F−centroid distances of 3.31 and 3.46 Å and shortest F−ring distances of 3.27 and 3.35 Å. In both sets of anion−π interactions, the more π-acidic pyrazolyl rings, rather than the linking arene rings, act as the electron-pair acceptors.

(b) Complexes of Bitopic Ligands: Coordination Polymers. Both $AgBF_4$ and $AgPF_6$ complexes of the *p*-phenylene-linked, bitopic ligand *p*-$[CH(pz)_2]_2C_6H_4$, **3** and **4**, crystallize as acyclic coordination polymers (Figures 7 and 8). The asymmetric unit of **3** comprises one silver cation, one-half each of two independent ligand molecules, and a disordered BF_4^- anion. The asymmetric unit of **4**·0.5CH_3CN contains two silver cations, one complete ligand molecule, and one-

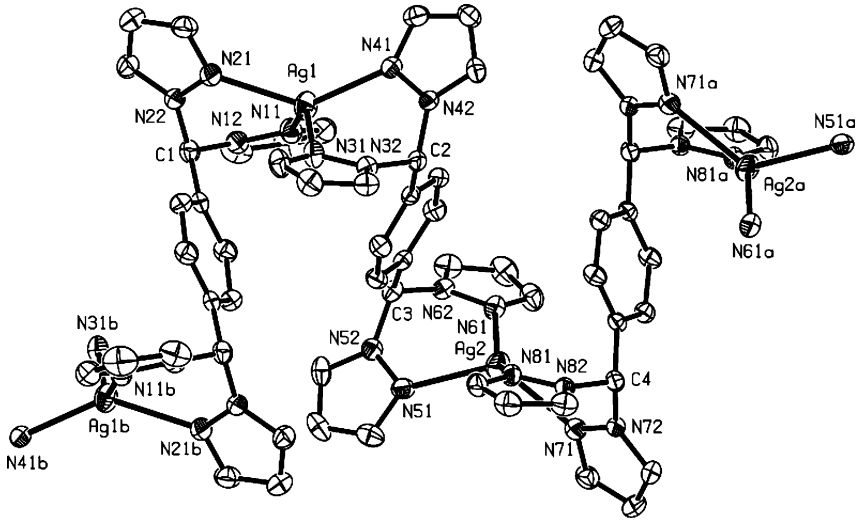

Figure 8. ORTEP drawing of the cationic coordination polymer in $\{[Ag(\mu\text{-}p\text{-}[CH(pz)_2]_2C_6H_4)_2]PF_6 \cdot 0.5CH_3CN\}_\infty$ (**4**·0.5CH_3CN). Displacement ellipsoids are drawn at the 50% probability level. Hydrogen atoms are omitted for clarity. Selected bond distances (Å) and angles (deg): Ag(1)−N(11) 2.304(2), Ag(1)−N(21) 2.331(2), Ag(1)−N(31) 2.370(2), Ag(1)−N(41) 2.293(2), Ag(2)−N(51) 2.346(2), Ag(2)−N(61) 2.290(2), Ag(2)−N(71) 2.355(2), Ag(1)−N(81) 2.306(2); N(11)−Ag(1)−N(21) 83.12(8), N(11)−Ag(1)−N(31) 136.94(9), N(11)−Ag(1)−N(41) 121.52(8), N(21)−Ag(1)−N(31) 105.74(8), N(21)−Ag(1)−N(41) 135.93(8), N(31)−Ag(1)−N(41) 81.36(8), N(51)−Ag(2)−N(61) 84.28(8), N(51)−Ag(2)−N(71) 124.00(8), N(51)−Ag(2)−N(81) 111.17(8), N(61)−Ag(2)−N(71) 110.45(8), N(61)−Ag(2)−N(81) 149.67(8), N(71)−Ag(2)−N(81) 83.12(8).

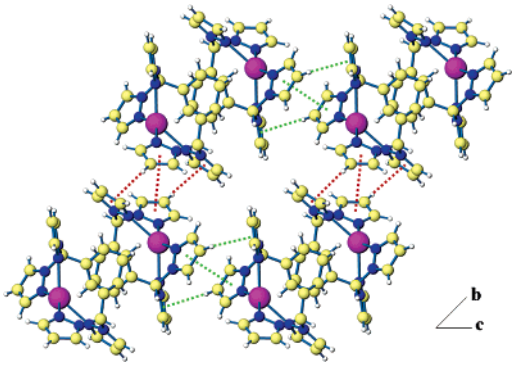

Figure 9. View down the chains of **3** showing two sets of quadruple pyrazolyl embrace interactions (red or green dashed lines).

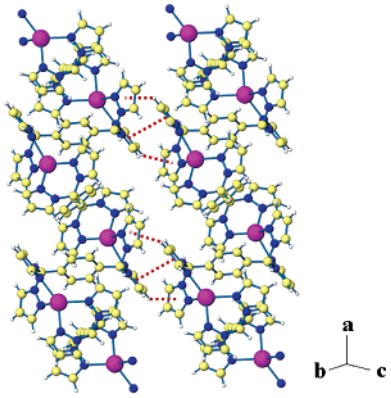

Figure 10. Parallel chains in **4**·0.5CH_3CN bridged by the quadruple pyrazolyl embrace (red dashed lines).

half each of two additional ligand molecules as well as two PF_6^- counterions and an acetonitrile molecule. The geometry about the silver is distorted tetrahedral with silver−nitrogen bond lengths and chelate ring bite angles comparable to those in the previous two complexes (2.28−2.39 Å and 81−84°). The cationic chains of both **3** and **4**·0.5CH_3CN are compact because of a tortuous propagation of the coordination polymers along the *a* axis in both structures.

The dominant feature of the supramolecular structures of both **3** and **4**·0.5CH_3CN is the quadruple pyrazolyl embrace,[5b] a concerted set of intermolecular CH−π and π−π interactions that associates the four pyrazolyl rings from two nearby bis(pyrazolyl)methane sites. This supramolecular motif is common in poly(pyrazolyl)methane and -borate compounds[5b] and illustrated here for both **3** and **4**·0.5CH_3CN (Figures 9 and 10). In the pyrazolyl embrace, two pyrazolyl rings are aligned for π−π stacking, and these two rings also act as hydrogen-atom donors, from their respective 4-pyrazolyl positions, in CH−π interactions involving the remaining two pyrazolyl rings. The structure of **3** contains two distinct sets of pyrazolyl embrace interactions, which correspond to the crystallographically independent ligand molecules and are shown in Figure 9 as red and green dashed lines, respectively. The interactions shown in red involve a centroid−centroid distance of 3.60 Å and CH−π distances of 2.67 Å. These interactions link the chains along the *b* axis. The interactions shown in green include a centroid−centroid distance of 3.56 Å and CH−π distances of 2.64 Å, and these interactions link the chains along the *c* axis. Since each set of interactions results in two-dimensional sheets of cationic polymers, the combined interactions produce a three-dimensional framework of these polymers. Beyond the pyrazolyl embrace, no significant noncovalent forces are evident in the crystal.

The crystal structure of **4**·0.5CH_3CN displays a supramolecular complexity similar to its meta counterpart, **2**. The pyrazolyl embrace, shown in Figure 10, is the most dominant feature with a centroid−centroid distance of 3.51 Å and CH−π distances of 2.80 and 3.00 Å. The sheets of cationic polymers formed by the embrace are expanded into an overall three-dimensional structure by a multitude of CH−F hydrogen bonds and anion−π interactions. The CH−F hydrogen bonds include as donors the pyrazolyl rings and the methine ($-CH(pz)_2$) units and are in the range of 2.2−2.5 Å. As

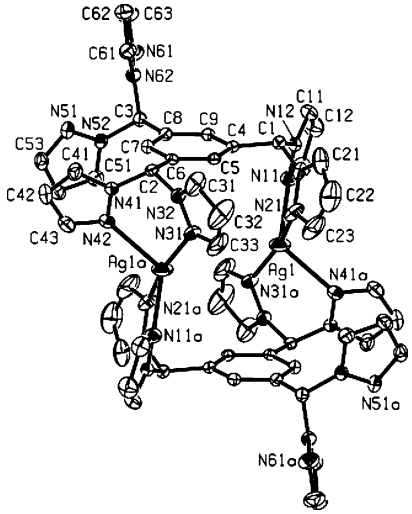

Figure 11. ORTEP drawing of the cationic unit in $[Ag_2(\mu\text{-}1,3,5\text{-}[CH(pz)_2]_3C_6H_3)_2](BF_4)_2$ (**5**). Displacement ellipsoids are drawn at the 40% probability level. Hydrogen atoms are omitted for clarity. Selected bond distances (Å) and angles (deg): Ag(1)−N(11) 2.363(2), Ag(1)−N(21) 2.269(3), Ag(1)−N(31a) 2.241(2), Ag(1)−N(41a) 2.393(2); N(11)−Ag(1)−N(21) 84.03(8), N(11)−Ag(1)−N(31a) 104.25(8), N(11)−Ag(1)−N(41a) 117.79(7), N(21)−Ag(1)−N(31a) 164.22(9), N(21)−Ag(1)−N(41a) 102.35(7), N(31a)−Ag(1)−N(41a) 85.85(7).

observed in **2**, the anion−π interactions are long (F−centroid distances 3.59 and 3.73 Å; F−ring distances 3.28 and 3.56 Å) and involve pyrazolyl rings but not the linking phenylene rings.

(c) Complexes of the Tritopic Ligand. Crystals of the complex $[Ag_2(\mu\text{-}1,3,5\text{-}[CH(pz)_2]_3C_6H_3)_2](BF_4)_2$ (**5**), resulting from the equimolar combination of $AgBF_4$ and the tritopic ligand $1,3,5\text{-}[CH(pz)_2]_3C_6H_3$ (**L**^{3}), consist of discrete dimeric argentacycles analogous to those in **1** and **2** except with a third bis(pyrazolyl)methane site that remains unbound. An ORTEP representation of the dicationic argentacycle in **5** is shown in Figure 11. The dication rests on an inversion center, and the third, unbound bis(pyrazolyl)methane units are diametrically arranged about the metallacycle. The geometry about the silver and bond lengths and angles in **5** are within the same ranges as those described for the previous four complexes.

The most notable features of the extended structure of **5** are the CH−π interactions that organize the complex ions into two-dimensional sheets in the *ac* plane. Figure 12 shows four molecules of **5** associated through CH−π interactions (purple dashed lines) where the hydrogen-atom donors are at the 5-position of metal-coordinated pyrazolyl groups and at the methine carbon atom. In both interactions, pyrazolyl rings from uncoordinated units serve as the hydrogen-atom acceptors. The 4-fold symmetry at the center of the grouping of ions in Figure 12 is apparent. Although the BF_4^- anions are ordered in this structure, no anion−π interactions are present, although several CH−F interactions (2.25−2.53 Å) do contribute to the three-dimensional supramolecular structure. Whereas the hydrogen-atom donors in the CH−π interactions do not include unbound pyrazolyl groups, the donors in the weak CH−F hydrogen bonds include both coordinated and uncoordinated pyrazolyl groups. Methine hydrogen atoms also take part in these CH−F interactions.

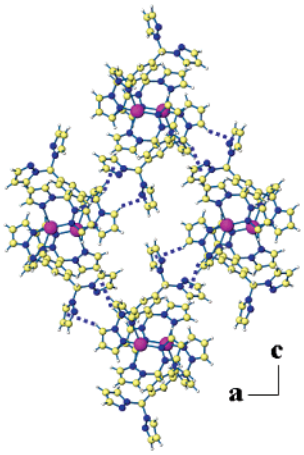

Figure 12. View down the *b* axis of **5** showing metallacycles associated through CH−π interactions (purple dashed lines).

Unique to this structure, because of the noncoordinated pyrazolyl rings, are CH−N interactions at 2.5−2.6 Å with the donors coming from the methine and coordinated pyrazolyl groups.

The complex $\{[Ag_3(\mu\text{-}1,3,5\text{-}[CH(pz)_2]_3C_6H_3)_2](BF_4)_3\cdot 2CH_3CN\}_\infty$ (**6**·$2CH_3CN$) results from reaction of an excess of $AgBF_4$ with **L**^{3}. It is the formal product of adding one more equivalent of $AgBF_4$ to bind the free bis(pyrazolyl)methane units of two complexes of **5** discussed above. An ORTEP drawing of **6**·$2CH_3CN$ (Figure 13) shows that the two bis(pyrazolyl)methane ligating sites that are unbound in **5** are coordinated to the additional silver cations in **6**·$2CH_3CN$ to yield a coordination polymer of metallacycles in which the additional silver ion bridges what are discrete metallacycles in **5**. All silver cations reside in distorted tetrahedral coordination environments similar to the other complexes reported here. The noncovalent interactions in **6**·$2CH_3CN$ resemble those in **5** in that CH−π interactions are the only strong forces between the argentacycles. In **6**·$2CH_3CN$ these multiple CH−π interactions bridge parallel chains of dications (Figure 14), resulting in a three-dimensional extended structure. This structure is also supported by various CH−F interactions (2.1−2.5 Å, not pictured). Unlike **5**, **6**·$2CH_3CN$ exhibits a weak anion−π interaction (F−centroid distance 3.77 Å; shortest F−ring distance 3.59 Å) between a fluorine atom in BF_4^- and a pyrazolyl ring coordinated to a bridging silver cation, but this anion−π interaction does not support the extended structure of **6**·$2CH_3CN$.

Discussion

Complex Structure in the Solid State. We previously showed that alkylidene-linked, bitopic bis(pyrazolyl)methane ligands (see Figure 1) are reliable synthons for building $[L_2Ag_2]^{2+}$-type metallacyclic structures.[5a,b] In the presence of weakly coordinating anions, all the alkylidene-linked ligands prefer to form these dimeric metallacycles rather than simple coordination polymers, regardless of the length of the spacer. Table 2 shows the Ag···Ag distances across the metallacycles formed using ligands with methylene, ethylene, and propylene spacers. The table also includes the corresponding average distances between methine carbon atoms in the

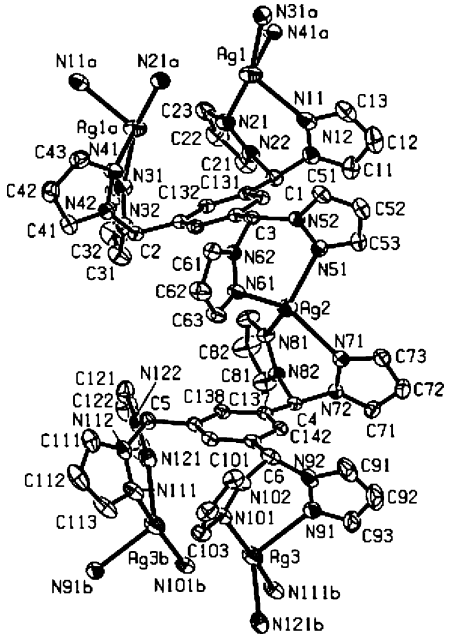

Figure 13. ORTEP drawing of a fragment of a chain of metallacycles in $\{[Ag_3(\mu\text{-}1,3,5\text{-}[CH(pz)_2]_3C_6H_3)_2](BF_4)_3\cdot 2CH_3CN\}_\infty$ (**6**·2CH_3CN). Displacement ellipsoids are drawn at the 50% probability level. Hydrogen atoms are omitted for clarity. Selected bond distances (Å) and angles (deg): Ag(1)−N(11) 2.361(2), Ag(1)−N(21) 2.289(2), Ag(1)−N(31a) 2.232(2), Ag(1)−N(41a) 2.5068(19), Ag(2)−N(51) 2.2963(19), Ag(2)−N(61) 2.3186(18), Ag(2)−N(71) 2.3832(19), Ag(2)−N(81) 2.2451(18), Ag(3)−N(91) 2.429(2), Ag(3)−N(101) 2.237(2), Ag(3)−N(111b) 2.251(2), Ag(3)−N(121b) 2.425(2); N(11)−Ag(1)−N(21) 86.73(7), N(11)−Ag(1)−N(31a) 109.31(7), N(11)−Ag(1)−N(41a) 104.44(7), N(21)−Ag(1)−N(31a) 162.95(7), N(21)−Ag(1)−N(41a) 87.11(7), N(31a)−Ag(1)−N(41a) 83.35(6), N(51)−Ag(2)−N(61) 84.83(6), N(51)−Ag(2)−N(71) 105.47(6), N(51)−Ag(2)−N(81) 138.64(7), N(61)−Ag(2)−N(71) 132.77(7), N(61)−Ag(2)−N(81) 116.88(7), N(71)−Ag(2)−N(81) 85.61(7), N(91)−Ag(3)−N(101) 85.16(7), N(91)−Ag(3)−N(111b) 98.23(7), N(91)−Ag(3)−N(121b) 114.55(7), N(101)−Ag(3)−N(111b) 167.99(8), N(101)−Ag(3)−N(121b) 104.17(7), N(111b)−Ag(3)−N(121b) 84.98(7).

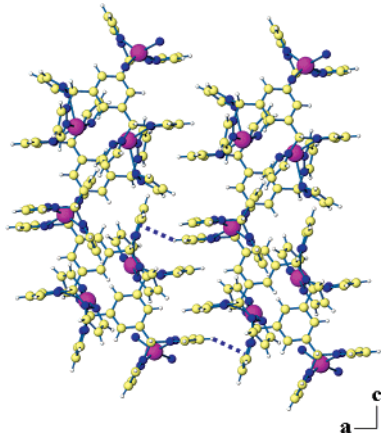

Figure 14. Fragments of parallel argentacyclic polymers in **6**·2CH_3CN, associated by a representative set of CH−π interactions (purple dashed lines).

ligand molecules within the metallacycles. The increase in Ag···Ag distance when lengthening the carbon chain from one to two, along with an increase in methine···methine distance, is expected given the natural increase in chain size and the propensity of the bis(pyrazolyl)methane groups to avoid steric crowding. Lengthening the spacer size from two to three, however, has a modest impact on the Ag···Ag distances, which are greater by no more than 0.4 Å, but has a greater effect on the methine···methine separations, which increase by approximately 1.2 Å. These trends show the expected flexibility of the propylene-linked ligand. The ethylene system can also be considered flexible because it has the freedom to alter the methine···methine distances, but when forming these types of metallacycles, this flexibility is greatly reduced.

Table 2. Comparison of Intraargentacyclic Distances in Complexes with Alkylidene-Linked Ligands, $[CH(pz)_2](CH_2)_n$[5a,b]

spacer size, *n*	Ag···Ag distance (Å)	methine···methine distance (Å)	counterion
1	4.34	2.52	$SO_3CF_3^-$
2	6.02	3.81	BF_4^-
	6.16	3.81	$SO_3CF_3^-$
3	6.16	5.00	BF_4^-
	6.42	5.02	$SO_3CF_3^-$

Table 3. Comparison of Torsion Angles and Intraargentacyclic Distances in Complexes with Fixed Ligands

compound	average torsion angle, τ (deg)	Ag···Ag distance (Å)	methine···methine distance (Å)
1·2$(CH_3)_2CO$·0.43H_2O	69	5.31	4.95
2	75	4.83	4.93
5	89	4.73	5.04
6·2CH_3CN[a]	92	4.24	5.07
	99	4.10	5.03

[a] Values given are for the two crystallographically distinct argentacycles present in the crystal.

Two questions prompted the use of arene spacers in the current work: would ligands with fixed distances between ligating groups, and therefore a greater degree of rigidity, also direct formation of dimeric metallacycles as in the alkylidene system and would the decrease in flexibility result in a greater impact of lengthening the spacer? To answer these questions we used the *meta*- and *para*-phenylene-linked ligands, $\mathbf{L}_m$ and $\mathbf{L}_p$, because they represent the simplest members of a family of arene-linked compounds comparable to the alkylidene-linked compounds studied previously. The tritopic ligand $\mathbf{L}^3$ is simply the bitopic ligand $\mathbf{L}_m$ with an additional ligating site that is meta to the other two sites. In changing from meta to para orientation about the phenylene ring the length of the spacer is effectively increased because the relative distances between ligating groups remain fixed at their respective meta or para distances.

As discussed above, the ligands $\mathbf{L}_m$ and $\mathbf{L}^3$, in which the ligating sites are oriented in a meta fashion about the arene linker, direct formation of silver metallacycles similar to those formed with the alkylidene ligands. The Ag···Ag distances in the four metallacyclic complexes, shown in Table 3, fall in the range 4.10−5.31 Å and more closely resemble the distance in the methylene-linked complex (4.34 Å) than they do the distances in the longer alkylidene systems (6.02−6.42 Å). The similarities between the methylene- and arene-linked systems support the intuitive conclusion that the methylene-linked compound, with only a single carbon atom spacer, is a fixed ligand as well, despite its chemical similarities to the flexible ethylene- and propylene-linked systems.

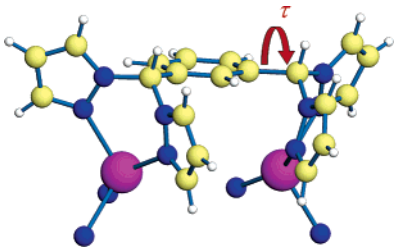

Figure 15. Illustration of the torsion angle, τ, for a silver(I) metallacycle (complete structure not shown).

The arene-linked ligands are best described as "fixed" but not necessarily "rigid" because although the relative distances between bis(pyrazolyl)methane ligating sites (the methine carbon atoms) remain essentially constant, rotation of the bis(pyrazolyl)methane units about the methine−arene carbon (ipso) bond allows variation in the way the ligands bind metal centers. For $\mathbf{L}_m$ and $\mathbf{L}^3$ this rotation can be quantified using the torsion angle, τ, which is defined as shown in Figure 15 as the torsion angle about the ipso and methine carbon atoms relative to the arene carbon atom that is ortho to both ipso carbon atoms and the methine hydrogen atom. For each metallacycle in this study, two of these torsion angles exist for both of the bitopic ligands $\mathbf{L}_m$ present. Because the coordinated metals are necessarily on the same side of the arene ring, the two values of τ in each ligand will be opposite in sign. The utility of τ arises from the fact that the greater the absolute value of τ, the closer the silver cations are to each other in the metallacycles.

Table 3 compares the average absolute values of the torsion angles for each metallacycle along with the respective Ag···Ag and methine···methine distances. The trend of increasing τ corresponding to decreasing Ag···Ag distance is clear, with the longest Ag···Ag distance (5.31 Å in **1**) being associated with the smallest torsion angle (69°) and the shortest Ag···Ag distance (4.10 Å in **6**) corresponding to the largest value of τ (99°). In contrast, the average methine···methine distance for all the complexes remains essentially constant, varying by no more than 0.14 Å. The distinction between "fixed" and "rigid" ligands is brought out clearly in our previous work with complexes such as $\{\mu$-*m*-$[CH(pz)_2]_2C_6H_4\}[Re(CO)_3Br]_2$ where the metals are on opposite sides of the arene linker. Such an arrangement of the silver(I) systems reported here would lead to coordination polymers, but we observe only metallacycles, demonstrating the tendency to form this type of structure with the meta ligands coordinated to metals that do not contain other ligands.

Changing from meta- to para-linked ligands has a dramatic effect on the solid-state structure as the metallacycles formed in complexes **1**, **2**, **5**, and **6** are replaced by coordination polymers in **3** and **4**. Although, as just described, some flexibility remains in these fixed systems, the greater stability of the polymers as compared to the macrocycles in the para-systems is attributed to the increased distance between ligating sites in $\mathbf{L}_p$ relative to $\mathbf{L}_m$. By increasing the distance between the methine carbon atoms from ca. 5 Å with $\mathbf{L}_m$ to 5.8 Å with $\mathbf{L}_p$ the latter ligand no longer favors formation of $[\mathbf{L}_2Ag_2]^{2+}$ metallacycles. Clearly, the greater rigidity built into these arene-linked ligands results in greater control of structure than with the alkylidene system reported earlier.

Recent work by Wagner[14] also suggests that *para*-phenylene-linked ligands analogous to *p*-$[CH(pz)_2]_2C_6H_4$ do not form stable metallacyclic dimers. The related bis(pyrazolyl)borate ligand $\{p$-$[B(pz)_2(^tBu)]_2C_6H_4\}^{2-}$ forms discrete chloride- and oxide-bridged complexes of titanium and manganese. Although two metals are coordinated in a fashion similar to complexes **1**, **2**, **5**, and **6**, only one ligand bridges the two metals rather than two, with the coordination environments of the metals usually completed by smaller ligands such as additional chloride ions, dimethylamide, or solvent molecules.

An interesting comparison of these compounds is with the those formed in similar reactions of $\mathbf{L}_m$ and $\mathbf{L}^3$ with BF_4^- salts of divalent iron, zinc, and cadmium.[15] These reactions also result in formation of metallacyclic dimers similar to the ones reported here but are accompanied by fluoride abstraction from one or two BF_4^- ions to yield the mono- or difluoride-bridged dimeric cations $[M_2(\mu\text{-}\mathbf{L}_m)_2(\mu\text{-F})](BF_4)_3$ (M = Fe, Zn), $[Cd_2(\mu\text{-}\mathbf{L}_m)_2(\mu\text{-F})_2](BF_4)_2$, and $[Zn_2(\mu\text{-}\mathbf{L}^3)_2(\mu\text{-F})](BF_4)_3$. The lower fluoride affinity of Ag^+, a softer ion than the divalent cations, and the generally lower coordination numbers found in silver(I) complexes reduce the impetus of Ag^+ to abstract fluoride from BF_4^-.

Complex Structures in Solution. Positive-ion electrospray (ESI(+)) mass spectrometry provides some indication of the solution structures of these complexes. The mass spectra of **1** and **2**, which exist as metallacycles in the solid state, show clusters of peaks corresponding to the dimeric metallacycles associated with one counterion, $[Ag_2(\mathbf{L}_m)_2X]^+$, as described in the Results section. The analogous peaks are not detected in solutions of **3** and **4**, which are acyclic polymers in the solid state. Other than the differences in base peak identities, these $[Ag_2(\mathbf{L}_m)_2X]^+$ dimeric peaks are the only distinction between the spectra of the metallacycles and those of the polymers. The ESI(+) mass spectra of the argentacycles reported here closely match the spectra from the argentacycles formed in the alkylidene-linked systems previously described[5a,b] in that the mass spectra of complexes that show the metallacycle in the solid state also have a peak assigned to the respective $[Ag_2L_2X]^+$ ions. Detection in the mass spectral experiments of clusters corresponding to the metallacycles for **1** and **2**, as well as for the alkylidene-linked systems, is not direct evidence for the presence of argentacycles in solution but does appear to provide a reliable measure for distinguishing complexes that in the solid state will form metallacycles from those forming acyclic species.

The discrete metallacycles of compound **5** and the polymeric metallacycles of **6**, both made from $\mathbf{L}^3$, also yield ESI(+) mass spectra suggestive of their solid-state structures. The spectra of **5** and **6** are identical in all but one respect. Both show the dimeric cation $[Ag_2(\mathbf{L}^3)_2BF_4]^+$ as well as the

(14) Bieller, S.; Bolte, M.; Lerner, H.-W.; Wagner, M. *Inorg. Chem.* **2005**, *44*, 9489.
(15) Reger, D. L.; Watson, R. P.; Gardinier, J. R.; Smith, M. D.; Pellechia, P. J. *Inorg. Chem.* **2006**, *45*, 10088−10097.

fragment $[Ag\mathbf{L}^3]^+$, but the spectrum of **6** also contains a cluster corresponding to the dimer associated with an additional $AgBF_4$ equivalent, $[Ag_3(\mathbf{L}^3)_2(BF_4)_2]^+$. It is possible, therefore, that in solution both compounds retain the metallacyclic structure and that for **6** at least some extended polymeric structure exists. In a general sense, the ESI(+) mass spectra of silver(I) complexes of our polytopic poly(pyrazolyl)methane ligands appear to parallel the solid-state structures.[5]

Solid-State Supramolecular Structure. The supramolecular structures of the silver complexes reported here exhibit a variety of weak hydrogen bonds, largely in the form of CH−π and CH−F interactions, as well as π−π stacking and anion−π interactions. The quadruple pyrazolyl embrace[5b] is present only in the coordination polymers **3** and **4**. Formation of the macrocycles, however, does not preclude the pyrazolyl embrace because it is observed in the macrocycle-containing structures of the alkylidene-linked ligands.[5a,b] Similarly, π−π stacking plays a limited role in the current study, and it is only present in the macrocyclic compound **2**, despite the intermolecular access to the central phenylene ring in **1** as well. It is not surprising that the winding polymers of **3** and **4** or the macrocycles of **5** and **6**, whose arene rings are partially blocked by another ligating group, do not allow π−π interactions in the solid state.

Full appreciation of the impact of the BF_4^- ions on the structure of **3** is hindered by disorder, but several weak CH−F hydrogen bonds are observed in the crystals of **1** (despite mild disorder in the anions), **5** and **6**. Similarly, the PF_6^- counterion in **2** and **4** also participates in several CH−F hydrogen bonds. Exploitation of noncovalent anion−π interactions in supramolecular chemistry is gaining ground on the more developed chemistry of cation−π interactions.[16] For example, Dunbar and co-workers recently published a thorough study of noncovalent anion−π interactions in AgX ($X = BF_4^-$, PF_6^-, AsF_6^-, SbF_6^-) complexes of the π-acidic ligands 3,6-bis(2′-pyridyl)-1,2,4,5-tetrazine (bptz) and 3,6-bis(2′-pyridyl)-1,2-pyridazine (bppn).[17] For our silver complexes reported here, anion−π contacts have been identified in **2**, **4**, and **6**, and the shortest F−centroid or F−ring plane distances are in the range of 3.2−3.8 Å. These interactions are long compared to the significant anion−π interactions reported in the recent literature, which tend to be below 3.0 Å.[17,18] All of the anion−π interactions observed here involve the pyrazolyl rings as the π acids, and this observation is consistent with the expected electron deficiency of the pyrazolyl group caused by the electron-withdrawing nitrogen atoms. The lack of a significant change in the chemical shifts of the BF_4^- and PF_6^- fluoride signals in the ^{19}F NMR spectra of the complexes reported here implies that no significant anion−π interactions exist in solution.[17]

Summary

The arene-linked ligands employed in this study form silver(I) complexes with consistent structures: dimeric metallacycles for ligands with a meta configuration and simple coordination polymers for the para configuration. These less flexible ligands in which the length of the spacer is fixed by the arene substitution do control the formation of metallacycles versus coordination polymers when compared to the more flexible alkylidene systems we reported earlier. Use of the tritopic ligand affords stoichiometry-dependent complexes containing either discrete dimeric metallacycles with equimolar amounts of silver salt and ligand or a polymer of metallacycles in the presence of an excess of silver salt. Weak noncovalent interactions supported by the functionality built into the ligands play an important role in the supramolecular structures of these complexes, and long anion−π contacts involving the relatively π-acidic pyrazolyl groups support the structures of some of these complexes. The results demonstrate that the series of bis(pyrazolyl)methane ligands we have been investigating, both alkylidene- and arene-based, increase the potential for the rational design of molecular and supramolecular structures, based on variations in cation and anion, as well as geometry and flexibility of the ligand.

Acknowledgment. We thank Drs. James Gardinier and Radu Semeniuc for helpful discussion and the National Science Foundation (CHE-0414239) for financial support. We also thank the Alfred P. Sloan Foundation for support of R.P.W. The Bruker CCD Single Crystal Diffractometer was purchased using funds provided by the NSF Instrumentation for Materials Research Program through Grant DMR: 9975623.

Supporting Information Available: X-ray crystallographic files in CIF format for all structures. This material is available free of charge via the Internet at http://pubs.acs.org.

IC0613053

(16) (a) Quiñonero, D.; Garau, C.; Rotger, C.; Frontera, A.; Ballester, P.; Costa, A.; Deyà, P. M. *Angew. Chem., Int. Ed.* **2002**, *41*, 3389. (b) Campos-Fernández, C. S.; Clérac, R.; Dunbar, K. R. *Angew. Chem., Int. Ed.* **1999**, *38*, 3477. (c) Campos-Fernández, C. S.; Clérac, R.; Kooman, J. M.; Russell, D. H.; Dunbar, K. R. *J. Am. Chem. Soc.* **2001**, *123*, 773. (d) Campos-Fernández, C. S.; Schottel, B. L.; Chifotides, H. T.; Bera, J. K.; Basca, J.; Kooman, J. M.; Russell, D. H.; Dunbar, K. R. *J. Am. Chem. Soc.* **2005**, *127*, 12909.

(17) Schottel, B. L.; Chifotides, H. T.; Shatruk, M.; Chouai, A.; Pérez, L. M.; Basca, J.; Dunbar, K. R. *J. Am. Chem. Soc.* **2006**, *128*, 5895.

(18) Fairchild, R. M.; Holman, K. T. *J. Am. Chem. Soc.* **2005**, *127*, 16364.